

ACCOUNT OF MULTIPLE SCATTERING EFFECTS DURING LIDAR SOUNDING OF CLOUD MEDIA

V.A. Korshunov

*Scientific-Production Company "Taifun",
USSR State Committee for Hydrometeorology, Obninsk
Received April 22, 1989.*

Approximate expressions for the contribution from multiple scattering (MS) to lidar returns from cloud media, which take account of the extinction coefficient profile along the beam path are obtained. An iterative algorithm is proposed for correcting the available single scattering solution of the lidar equation for MS effects. An algorithm is described for interpreting lidar returns which yields the optical thickness m and the extinction coefficient profiles for cloud layers of $1.5 \leq \tau \leq 6$ for a set of lidar returns corresponding to different receiver fields of view. The same detector scheme is shown to be capable of retrieving profiles of the integral parameters of the cloud particles size spectrum and the liquid water content of the cloud.

Backscattered signals obtained during lidar sounding of cloud media generally contain a significant fraction of multiply scattered radiation.

In principle two approaches to the interpretation of such signals for which the multiple scattering (MS) contribution is large are possible. The first is to account for the MS effects in order to be able to exclude them and to use well-known techniques developed for the single-scattering approximation for further processing of the signals.^{1,2} Such an approach is quite difficult: indeed, the values of the corrections themselves depend upon the optical characteristics of the medium and on the parameters of the particle size spectrum. The latter, in their turn, are a priori unknown, and must in general be retrieved from the lidar returns. So far no practically acceptable techniques have been developed for such an account of MS.

The second approach to interpreting lidar returns from cloud media proposes not only to eliminate the MS effects, but also to make use of the information contained in the MS component of the signal. As an example of such an approach, consider the technique proposed in Ref. 3 for determining the optical and geometrical thicknesses of a homogeneous cloud. Attempts to outline possible methods for such a use of MS effects were undertaken in a number of other studies (see, e.g., Refs. 4 and 5). However, no significant progress has been achieved so far in this direction, either.

The present study proposes, on the basis of results from Ref. 6, an algorithm to account for MS contributions during conventional single-scattering processing of lidar returns. The study also examines possible ways of employing MS effects to retrieve the extinction coefficient profile and the integral parameter of the cloud particle size spectrum.

CALCULATION OF THE MS CONTRIBUTION TO LASER RETURNS: CONSTRUCTION OF APPROXIMATE RELATIONSHIPS

When constructing algorithms to account for the MS contributions to lidar returns, one first of all needs to develop a simplified procedure by which to calculate the MS contribution $\lg P/P_1$. Here P is the signal power due to the MS contribution, and P_1 is the single-scattering component of the signal. Such a step is needed since direct application of the well-known Monte-Carlo techniques or of the small-angle approximation to the running auxiliary calculation would be impractical because of the large amount of computer time that would be needed.⁷ It is therefore proposed to use certain relationships derived in advance and approximating the results of exact calculations. Below we examine one possible option for constructing such relationships.

Let us assume that the receiving angles used are wide enough so that the MS contribution depends only weakly on the particle size.⁶ Restricting our treatment to the case in which the cloud-to-laser distance z_0 is sufficiently large, we can regard the source and the receiver as point-size, spatially coincident objects. Assume further that the source divergence angle is several times less than the receiving angle $2\varphi_r$ and that the extinction coefficient within the cloud layer $\sigma(z)$ depends only on the distance along the sounding beam path z . It was shown in Ref. 8 that within the accuracy of the approximations the form of the functional dependence of $\lg P/P_1$ on the receiving angle is practically identical for both homogeneous and inhomogeneous layers. It was also proposed there to introduce an effective parameter τ_{0ef} , thus reducing the general case of arbitrary $\sigma(z)$ to that of a homogeneous layer with $\tau_0 = \sigma_0 z = \tau_{0ef}$.

It is advisable by way of introducing τ_{0ef} to treat first the particular case of extremely wide receiving angles; quite simple analytical formulas can be obtained for it within the small-angle approximation.⁷ (The applicability of the technique from Ref. 7 for calculating P/P_1 in the case of sufficiently wide receiving angles was demonstrated in Ref. 9).

Starting from the relations for P/P_1 obtained in Ref. 7, and assuming in addition that the thickness of the sounded layer $z - z_0$ is small in comparison with z , one can obtain the following formula for large φ_r :

$$\frac{P}{P_1} = \frac{1}{8\pi} \int_0^\infty dp q_\pi(p) p \exp[4\pi\tau q(p)] \times \left\{ 1 - \exp \left[\varphi_r^2 \left[8\pi \frac{dq}{dp} p^{-1} \cdot \int_{z_0}^z \sigma(\eta) \left(1 - \frac{\eta}{z} \right)^2 d\eta \right]^{-1} \right] \right\} \quad (1)$$

where $q(p)$ and $q_\pi(p)$ are the Hankel transforms of the small-angle scattering phase functions in the forward ($g(\gamma)$) and backward ($g_\pi(\gamma)$) directions, so that

$$g_\pi = g_\pi(0) = \int_{z_0}^z \sigma(\eta) d\eta.$$

It can be seen from formula (1) that at large φ_r the functional relation between P/P_1 and $\sigma(z)$ is manifested in explicit form through the integral term

$\int_{z_0}^z \sigma(\eta) \left(1 - \frac{\eta}{z} \right)^2$. Taking this type of functional dependence as basic, we can introduce the effective parameter

$$\tau_{0ef} = \frac{z_0(z - z_0)\tau(z)^2}{3z^2 \int_{z_0}^z \sigma(\eta) \left(1 - \frac{\eta}{z} \right)^2 d\eta} \quad (2)$$

As seen from Eq. (2) the expression for τ_{0ef} yields the correct value of $\tau_0 = z_0\sigma$ for $\sigma(z) = \sigma \equiv \text{const}$.

Comparing these results with those calculated from the formulas given in Ref. 7, one can see that the applicability range of formula (1) is rather narrow. Indeed, at an accuracy level not worse than 10% formula (1) is applicable to a homogeneous layer with $\tau_0 = 10$ and $\tau = 4$, but only if $\varphi_r > 10^\circ$. Therefore direct use of formula (1) for calculations of P/P_1 is inadvisable. Meanwhile, numerical analysis shows that the relation (2), derived from relation (1), can be used well outside the applicability limits of formula (1), that is, for considerably lower values of φ_r . We only have to calculate P/P_1 for a homogeneous layer using the exact formulas. In particular it was shown that if the calculations are made separately for linear and exponential profiles of $\sigma(z)$, and for a homogeneous layer with the corresponding τ_{0ef} ($\tau_0 = 10, \tau \leq 4$), the difference in the magnitude of the MS contribution should not exceed 7% for $\varphi_r = 12'$, and 15% for $\varphi_r = 2'$.

TABLE I.

Approximation coefficients (angular minutes).

φ_r ang. min.	a_1	a_2	a_3	a_4	a_5	a_6
4	2.111-02	6.593-02	5.425-02	4.821-03	-1.432-02	4.502-03
6	2.827-02	1.284-01	2.687-02	7.654-03	-2.065-02	8.100-03
12	6.922-02	1.841-01	-9.732-03	1.099-02	-2.583-02	1.165-02
20	1.286-01	1.841-01	-1.037-02	1.074-02	-2.162-02	1.053-02
30	1.854-01	1.436-01	3.294-03	9.725-03	-1.518-02	8.124-03
60	2.680-01	9.258-02	1.842-02	1.057-02	-9.344-03	6.524-03
150	3.367-01	4.054-02	6.114-02	1.656-02	-3.278-03	1.086-03
300	3.760-01	9.465-02	1.565-02	2.251-02	-1.161-02	8.486-03
600	4.332-01	1.382-01	-6.107-02	2.591-02	-1.497-02	1.603-02

Having introduced τ_{0ef} we now must turn to the construction of formulas that approximate the MS contribution from a homogeneous layer as a function of the parameters τ and τ_0 . These indeed determine the MS contribution from a homogeneous layer for a given φ_r . It was found that a quite satisfactory approximation is given by the relation

$$\ln P/P_1 = (a_1 + a_2 y + a_3 y^2)\tau + (a_4 + a_5 y + a_6 y^2)\tau^2 \quad (3)$$

where $y = \lg \tau_0$.

The coefficients $a_1 - a_6$, which depend on φ_r , are found by the method of least squares. The respective values for a C1 cloud scattering phase function

($\lambda = 0.532 \mu\text{m}$) obtained for certain receiving angles are presented in Table I. The rms error produced by the approximate relation (3) reaches 0.02–0.03 for $\tau = 0-6$ at $\varphi_r \leq 60'$ for $\tau_0 = 1-100$ and 0.02–0.04 at $\varphi_r > 60'$ for $\tau_0 = 1-20$.

**RETRIEVAL OF THE CLOUD MEDIUM
EXTINCTION COEFFICIENT:
ACCOUNT OF THE MS CONTRIBUTION**

Using the above approximate relations we can account for the MS contribution while simultaneously using single-scattering techniques to determine $\sigma(z)$. Let us consider, by way of an example, a computational procedure for estimating the MS contribution to the well-known solution of the lidar sounding equation. It is derived on the assumption of the constancy of the lidar ratio along the beam path, so that the value $\sigma(z^*)$ at some point z^* at the end of the beam path is taken as a boundary condition. The point z^* is automatically assumed to be located inside the cloud, and the value $\sigma(z^*)$ a priori to be equal to some characteristic value of the cloud medium σ^* .² The relation for $\sigma(z)$ in that case can be written as

$$\sigma(z) = \hat{P}(z)R(z)^{-1} \left[\hat{P}(z^*)R(z^*)^{-1} \cdot \frac{1}{\sigma^*} + 2 \int_z^{z^*} \hat{P}(z')R(z')^{-1} dz' \right], \tag{4}$$

Here $\hat{P}(z)$ is the lidar return multiplied by z^2 , and $R(z) = P(z)/P_1(z)$.

Retrieval of $\sigma(z)$ from Eq. (4), which takes MS into account, follows the iterative scheme described below. It is assumed for the first step that $R^{(1)}(z) \equiv 1$, and $\sigma^1(z)$ is found from Eq. (4). Then, during the second iteration the value of $R^{(2)}(z)$ is found using Eqs. (2) and (3). Substituting it into Eq. (4), we obtain $\sigma^{(2)}(z)$; the process is continued until the values of $\sigma^{(k)}(z)$ obtained from successive iterations begin to differ only infinitesimally from each other. Numerical experiments with some typical profiles of $\sigma(z)$ encountered in lower cloud layers confirm that this iterative procedure converges to the true values.

**RETRIEVAL OF THE CLOUD LAYER
OPTICAL THICKNESS AND EXTINCTION
COEFFICIENT PROFILE**

In case of sounding of a cloud layer of comparatively low optical thickness ($\tau \leq 6$), the point z^* can lie close to the layer boundary farthest from the lidar. An a priori choice of $\sigma(z^*)$ then becomes impossible. In that case it is suggested to treat the value of $\sigma(z^*)$, or some alternative constant playing the role of boundary condition, as an unknown parameter. To determine it, it is necessary to make use of additional

experimental data, so several signals corresponding to various receiving angles must be recorded simultaneously.

It is expedient to choose as such a parameter the optical thickness of the cloud layer along the beam path $\tau = \int_{z_0}^{z^*} \sigma(z) dz$. Then, similar to relation (4), the solutions of the lidar equation corresponding to various receiver fields of view, written for $\sigma(z)$, are written in the following form:

$$\sigma(z) = 0.5 \hat{P}_1(z)R_1(z)^{-1} \left[T \int_{z_0}^z \hat{P}_1(z')R_1(z')^{-1} dz' + \int_z^{z^*} \hat{P}_1(z')R_1(z')^{-1} dz' \right], \tag{5}$$

where

$$T = \exp(-2\tau) [1 - \exp(-2\tau)]^{-1},$$

$$R_1(z) = P_1(z)/P_{11}(z), \quad i = 1, 2, \dots, N_r$$

is the number of returns received.

To determine τ and $\sigma(z)$ from Eq. (5) we consider an algorithm which combined the iterative procedure for determining $\sigma_1(z)$ described in the previous section with the procedure of minimizing over τ . The algorithm begins by prescribing some starting value of $\tau = \tau_N$ which, generally speaking, does not coincide with the unknown true value $\tau = \tau_{\text{true}}$. For each signal $\hat{P}_1(z)$ the above-described iterative procedure is performed and the profile of $\sigma_1(z)$ is retrieved from relation (5). The profiles of $\sigma_1(z)$ thus obtained will, in general, differ. Let us introduce a profiles discrepancy function

$$F(\tau) = \sum_{i=1}^N \sum_{k=1}^{N_t} [\sigma_1(z_k) - \bar{\sigma}(z_k)]^2, \tag{6}$$

where z_k is a set of N_t grid points selected from the segment $[z_0, z^*]$, such that

$$\bar{\sigma}(z_k) = \frac{1}{N_p} \sum \sigma_1(z_k).$$

In the absence of both computational and experimental errors, the function $\Phi(\tau)$ has a local minimum at $\tau = \tau_{\text{true}}$. Therefore, by minimizing $\Phi(\tau)$ as a function of τ using one of the well known techniques (we employed the "golden section" technique¹⁰) one can obtain the desired value of the layer optical thickness. The value of $\sigma(z) = \bar{\sigma}(z)$ can be taken as the solution for the extinction coefficient profile.

To determine the level of conditioning of this problem, certain numerical experiments were per-

formed. We assumed different levels of experimental and systematic error. In order to determine the effect of experimental errors, the contribution of calculational errors was excluded by using instead of the exact formulas approximate relations (2) and (3) to calculate the MS in the modeled experimental returns.

During the numerical experiments the shape of the $\sigma(z)$ profile was varied as well as the signal wavelength and the receiving angle. The number of receiving angles N_r was taken to be equal to two or three. Typical examples of the profiles used are shown in Fig. 1. The initial distance z_0 was 2, 4, 3, and 0.4 km for profiles 1, 2, 3, and 4, respectively.

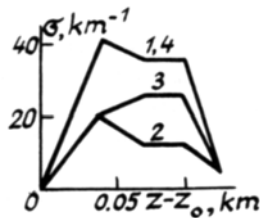


FIG. 1. Extinction coefficient profiles

Analysis of the result obtained demonstrates that for a prescribed level of experimental error and a given ϵ , the rms error values $\epsilon_\tau = \sqrt{\Delta\tau^2}$ and $\epsilon_{\sigma_k} = \sqrt{\Delta\sigma_k^2}$ weakly depend on the signal wavelength and the profile shape. Parameters decisive for the error level are τ and the range of receiving angles, the latter given by the ratio of the maximum to the minimum receiving angle T_ϕ . At higher T_ϕ both errors ϵ_τ and ϵ_{σ_k} decrease. An account of the factors which limit the range of T_ϕ demonstrated the angle range optimal for our purposes to be $\phi_r = 1^\circ - 10^\circ$ for $\tau_0 \leq 10$. Correspondingly, when $\tau_0 > 10$, the optimal ϕ_r starts to decrease in inverse proportion to τ_0 .

Table II presents the results of numerical experiments with values of $\sigma(z)$ shown in Fig. 1 at the optimal receiving angles. The error ϵ_{σ_k} is given for the farthest beam path point z^* , where it reaches its maximum.

TABLE II.

Results of numerical experiments

Model No.	τ	ϕ_r , angular minutes	ϵ	ϵ_τ	ϵ_{σ^*}
1	3.52	6, 12, 60	0.15	0.11	0.29
1	3.52	6, 60	0.15	0.13	0.32
4	3.52	6, 600	0.15	0.14	0.32
3	2.24	6, 12, 60	0.10	0.15	0.28
2	1.49	6, 12, 60	0.10	0.25	0.43

It can be seen from Table II that the errors ϵ_τ and ϵ_{σ^*} increase with decreasing τ . The cause for such a strong dependence of the errors on the parameter τ and T_ϕ is that the latter determine the difference in the MS

contribution (and, respectively, in the returns) for different receiving angles. It is this difference which plays the role of the Informative value with respect to τ . When τ and T_ϕ decrease, this difference also decreases, which results in the growth of ϵ_τ and ϵ_{σ_k} . Numerical experiments demonstrate that for sensible values of ϵ the errors ϵ_τ and ϵ_{σ_k} sharply increase for $\tau \approx 1$; moreover, in certain cases the minimum in $\Phi(\tau)$ is generally absent within the range of physically acceptable values of τ (the so-called solution breakdown); therefore the value $\tau \approx 1 - 1.5$ is the lower applicability limit for this technique.

The approximations on which the model is based are of the source of the systematic errors. That is why the calculations of the MS contribution to the "experimental" returns were performed using the exact relations (7) for a prescribed variation of the spectrum along the beam path. This study demonstrates that for $c = 0.15$ the effect of systematic errors is comparable to that of the experimental ones. If experimental errors are kept below 10% ($\epsilon \leq 0.10$), which however is difficult to maintain (recalling the wide range of signal variation), it makes sense to refine the technique of approximate MS calculations.

JOINT RETRIEVAL OF THE PARTICLE SIZE SPECTRUM INTEGRAL PARAMETER AND THE EXTINCTION COEFFICIENT PROFILES

The conditions for posing this problem were discussed in Ref. 6. Let us consider one way of constructing an algorithm for inverting sensing data taken with various values of the receiver aperture angle for the profiles of the particle size spectrum integral parameter $r_n(z)$ and the extinction coefficient $\sigma(z)$. This algorithm has a preliminary model character and it assumes that within every segment of the beam path $[z_{j-1}, z_j]$ the value of $\sigma(z)$ varies from σ_{j-1} to σ_j linearly and the parameter r_{nj} remains constant on $[z_{j-1}, z_j]$.

The set of initial data consists of N_s lidar returns $F(z, \phi_1)$ which correspond to receiving angles ϕ_1 , chosen following the recommendations of Ref. 6. The signals $F(z, \phi_1)$ are assumed not to have any absolute calibration, i.e., they are known only to within some arbitrary constant factor. The proposed algorithm performs successive retrieval of σ_j and r_{nj} starting with $j = 1$. The value of σ_0 is taken to be known (since the point z_0 lies at the layer boundary, to determine σ_0 one can apply the techniques described in Ref. 1).

Transfer from one interval of the partitioned beam path to the next follows the scheme presented below. Let the quantities σ_k and r_{nk} be already determined for $k \leq L - 1$. Then the quantities σ_L and r_{nL} can be treated as unknown parameters subject to retrieval within the interval $[z_{L-1}, z_L]$ under the condition of best agreement with the experimental $F(z, \phi_1)$ and calculated $F_L(z, \phi_1)$ returns. We introduce the signal discrepancy function for $F(z, \phi_1)$ and $F_L(z, \phi_1)$

$$F(\sigma_L, r_{nL}) = \sum_{m,1} [C_1 F_t(\sigma_L, z_{nL}, z_m, \varphi_1) - F(z_m, \varphi_1)]^2, \tag{7}$$

where $\{z_m\}$ is some set of points from the interval $[z_{L-1}, z_L]$ and C_1 are unknown constants. Our task now obviously consists in finding the values of σ_L, r_{nL} , and C_L that minimize $\Phi(\sigma_L, r_{nL})$. It can be shown that this minimum in the parameter C_1 is reached when

$$C_1 = \left(\sum_{m,1} F_t F \right) \left(\sum_{m,1} F_t^2 \right)^{-1}. \text{ Therefore our task is reduced}$$

to minimizing $\Phi(\sigma_L, r_{nL})$ in the space σ_L, r_{nL} for the above values of C_1 . Such a minimization is performed applying the available nonlinear parameter optimization techniques.¹⁰

Since the MS contribution for selected φ_r depends on r_n , only the particle spectrum shape was fixed during our calculations (the gamma distribution with $\mu = 6$ was chosen). Its modal radius, uniquely related to r_n , served as the free parameter. The values of $F(z, \varphi_1)$ were calculated according to the exact relations given in Ref. 7. To reduce the amount of needed computer time, our computational scheme assumed the exact calculation of $\lg P/P_1$ for some specified set of grid points in the σ, r_n plane and quadratic interpolation at the points in-between. This set of grid points was shifted to follow the optimization algorithm in its movement to the point of minimum.

Examples of the application of the above-described algorithm are given in Fig. 2. The solid curves represent the given profiles and the dashed curves – the retrieved profiles of $\sigma(z)$ and $r_{32}(z)$. Four different reception angles were considered in Fig. 2a: $\varphi_1 = 2', 4', 6',$ and $8'$, and five in Fig. 2b: $\varphi_1 = 2', 4', 6', 10',$ and $16'$. The particle size spectra for the individual intervals $[z_{j-1}, z_j]$ were taken to be uni- and bimodal functions, made up from log-normal and gamma-distributions. The modal radii of the individual modes remained within the limits 1–6 μm except for the first interval (see Fig. 2a) where they are equal to 0.15 and 1.5 μm .

Figure 2 demonstrates quite satisfactory agreement between the given profiles and those retrieved from the lidar returns. The discrepancies result both from computational error and from the effects of the initial approximations (namely, the correlation assumed between $\lg P/P_1$ and r_{32}) introduced in the statement of the problem.⁶

Summing up the results of the given study in combination with those of Ref. 6, we note that ac-

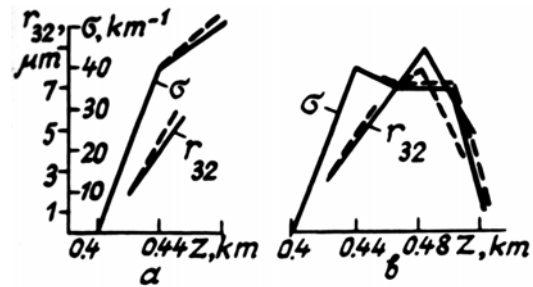


FIG. 2. Examples of retrieval of the extinction coefficient profiles and the integral parameter r_{32} of the particle size spectra $\sigma(z)$ (numerical experiment).

counting for the effects of MS makes it possible to considerably broaden the capabilities of lidar sounding of cloud media, in particular – to go to greater optical thicknesses, at least up to $\tau = 6$ when determining the extinction coefficient profile, and also to perform throughput lidar sounding of cloud layers with retrieval of their optical thickness ($1.5 \leq \tau \leq 6$). The fundamental possibility of retrieving the profiles of the integral size parameter and the cloud medium water content has also been demonstrated.

REFERENCES

1. V.E. Zuev, G.M. Krekov, M.M. Krekova, et al., *Problems of Lidar Sounding of the Atmosphere*, Nauka, Novosibirsk (1976).
2. V.E. Zuev, G.O. Zadde, S.I. Kavkyanov, et al., *Remote Sensing of the Atmosphere*, Nauka, Novosibirsk (1978).
3. V.V. Belov and G.N. Glasov, *Lidar Sounding of Geometrical and Optical Cloud Thicknesses*, Preprint No. 16, Institute of Atmospheric Optics, Siberian Branch of the Academy of Sciences of the USSR. Tomsk (1976).
4. B.V. Kaul', G.M. Krekov, and M.M. Krekova, *Kvant. Elektron.* **4**, No. 11. 2408 (1977).
5. V.S. Shamaev, in: *Abstracts of Reports at the the Sixth All-Union Symposium on Laser and Acoustic Sensing of the Atmosphere*. Part I, Tomsk (1980).
6. V.S. Korshunov. *Atm. Opt.* **3**, No. 1, 5 (1990).
7. V.S. Korshunov, *Izv. Vyssh. Uchebn. Zaved., Ser. Radiofiz.* **24**, No. 9. 1099 (1980).
8. V.S. Korshunov, *Trudy IEM*, No. 45 *Gidrometeoizdat*, Moscow (1988).
9. V.S. Korshunov, *Izv. Vyssh. Uchebn. Zaved., Ser. Radiofiz.* **30**, No. 10. 1193 (1987).
10. F. Gill, W. Murray and M. Wright, *Practical Optimization* (Russian translation] (Mir, Moscow, 1985).